

Reliability of flip-chip bonded RFID die using anisotropic conductive paste hybrid material

Jun-Sik LEE¹, Jun-Ki KIM¹, Mok-Soon KIM², Namhyun KANG³, Jong-Hyun LEE⁴

1. Advanced Joining Technology Team/Microjoining Center, Korea Institute of Industrial Technology(KITECH), Yeonsu-gu, Incheon 406-840, Korea;

2. School of Materials Science & Engineering, Inha University, Incheon 402-020, Korea;

3. Department of Materials Science & Engineering, Pusan National University, Busan 609-735, Korea;

4. Department of Materials Science & Engineering, Seoul National University of Technology, Seoul 139-743, Korea

Received 21 April 2010; accepted 10 September 2010

Abstract: A reliability of flip-chip bonded die as a function of anisotropic conductive paste (ACP) hybrid materials, bonding conditions, and antenna pattern materials was investigated during the assembly of radio frequency identification(RFID) inlay. The optimization condition for flip-chip bonding was determined from the behavior of bonding strength. Under the optimized condition, the shear strength for the antenna printed with paste-type Ag ink was larger than that for Cu antenna. Furthermore, an identification distance was varied from the antenna materials. Comparing with the Ag antenna pattern, the as-bonded die on Cu antenna showed a larger distance of identification. However, the long-term reliability of inlay using the Cu antenna was decreased significantly as a function of aging time at room temperature because of the bended shape of Cu antenna formed during the flip-chip bonding process.

Key words: RFID inlay; ACP; flip-chip, bonding process; reliability

1 Introduction

Recently, the radio frequency identification(RFID) technology is anticipated to be used everywhere in our life because the production cost is significantly improved to be competitive[1]. The improvement of the production cost is realized due to the mass production. One of the representative mass production is R2R (roll-to-roll or reel-to-reel) method[2]. The R2R method should be applied to die bonding and converting as well as antenna printing[2–3]. Anisotropic conductive paste (ACP) or isotropic conductive paste (ICP) are used to conduct die-bonding process through R2R method[2–13]. The ACP and ICA are metal/polymer hybrid materials and heat-curable conductive adhesives.

The RFID industry recently requires the ACP of rapid curing properties. This is because the decrease of die-bonding time directly reduces the production cost of RFID tag[2]. If the curing time is not enough to be optimized, however, the quality of RFID inlay is deteriorated. Therefore, the performance variation and bonding reliability should be investigated as a function

of ACP materials and curing condition to determine fast and reliable assembly condition of RFID inlay. Nevertheless, the ACP studies used for RFID die-bonding process were very rare, specifically to the flexible substrate such as polyethylene terephthalate (PET) as far as the authors recognized.

This study performed the die-bonding process by using ACP on PET substrate and investigated the bonding reliability for RFID application. The method for producing antenna pattern is rapidly changing from the established etching of Cu foil to the paste-type Ag ink or nano Ag ink[14–17]. Compared with the Cu antenna, the Ag antenna should show significantly different properties because the printed Ag ink has its own electrical resistivity and the different prominence in the pattern surface. For the reason, this study conducted the die-bonding process and reliability test as a function of different materials for the antenna.

2 Experimental

This study investigated the behavior of shear bonding strength and recognition distance as a function

different materials for the antenna.

2 Experimental

This study investigated the behavior of shear bonding strength and recognition distance as a function of antenna materials and ACP curing conditions. The microstructure in the joint for each curing condition was measured by using scanning electron microscope (SEM). The long-term reliability for the flip-chip joints was tested through checking the variation of recognition distance as the RFID inlay was aged for 1 month at room temperature.

2.1 Parts and materials

Model of used RFID chips was RI-UHF-00001 of Texas Instrument, USA. The dimension of the RFID chip was $865\ \mu\text{m} \times 780\ \mu\text{m} \times 140\ \mu\text{m}$ and the height of Au bumps was $20\ \mu\text{m}$. The antenna patterns were formed on PET film by using two materials: Cu foil and paste-type Ag ink (model: Parmod[®] ink, Parelec, Germany).

The used ACPs were also two models. Table 1 shows the characteristics of ACP-1 (MONOPOX_AC163, Delo, Germany) and ACP-2 TAP0402E, Kyocera, Japan). ACP-1 needs curing time of 6–19 s at 150–210 °C and ACP-2 needs 2–5 s at 180 °C. For the conducting filler materials in ACP, ACP-1 used Ag powder (3 μm in diameter) and ACP-2 utilized polymer particle coated with Au/Ni (3 μm in diameter), respectively, and the shape was spherical. Differential scanning calorimeter (DSC) measured the behavior of exothermic peaks with respect to heating rates for analyzing the curing behavior of ACP. Several studies reported that the DSC peaks are very sensitive to the amount of materials measured[18]. Therefore, the amount of ACP used for DSC was maintained to be constant (7 mg) for improving the experimental accuracy and reproducibility.

2.2 Bonding process for RFID die

Figure 1 shows the schematic diagram of flip-chip bonding process for RFID dies. The antenna patterns were produced on the substrate (PET). The flip-chip bonder (model: Fineplacer[®], Finetech, Germany) picked up the RFID die and arrayed the pad of antenna pattern

with the bump of RFID die. Prior to contact, the dispenser applied 2.5 mL of ACP as a glob-top shape on the antenna pad, therefore covering all 4 pads on the antenna pattern at a time. And then, a thermo-compression bonded the RFID die to the pad of the antenna pattern.

The initial temperature of the bottom plate under the antenna pattern was set to 120 °C and that of the hot bar to press the chip was set to 150 °C. The maximum temperatures for the bottom plate and hot bar were set to 150 and 180 °C, respectively. To reduce the bonding

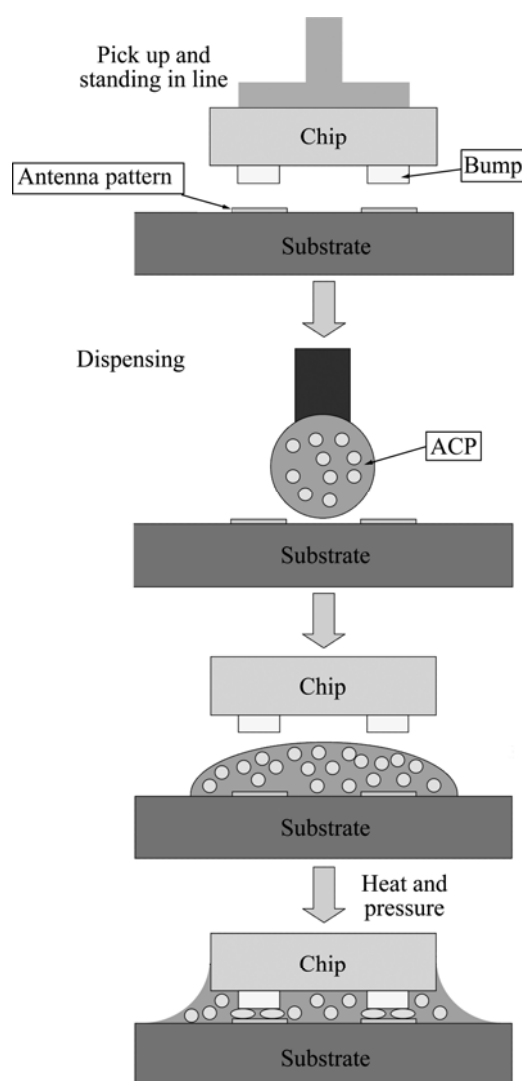


Fig.1 Schematic diagram of flip-chip bonding process for RFID

Table 1 Properties of ACP materials studied

Bonding material	Model	Viscosity/ (Pa·s)	Filler composition	Suggested curing time/s	Suggested bonding pressure	$t_g/^\circ\text{C}$	Elastic modulus/GPa
ACP-1	MONOPOX AC163	30(at 23 °C)	Ag particle (dia. $\approx 3\ \mu\text{m}$)	6–19(at 150–210 °C)	0.392–1.078 N per bump	135	3.3
ACP-2	TAP0604C	25(at 25 °C)	Au/Ni coated polymer particle (dia. $\approx 3\ \mu\text{m}$)	15–20(at 150 °C), 2–5 (at 180 °C)	0.294–1.176 N/ 100 μm per bump	110	3.0(at 25 °C)

time, the bonder was designed to increase temperature rapidly from the initial temperature to the maximum temperature. Therefore, a variable for the bonding process was the bonding time that was set to every 5 s step between 4 and 15 s.

Figure 2 indicates the temporal behavior of the hot bar and the bottom plate as a function of bonding time. As the bonding time reached to 7 s and 10 s, the temperature of the hot bar and the bottom plate increased to the maximum temperature, respectively. Therefore, as the bonding time exceeded over approximately 10 s, the process temperature was maintained very stably at the maximum temperature. The appropriately large compressive force applied to the bonding process of ACP deformed sufficiently the fillers, therefore improving the reliability of the joints[19]. For the reason, the compression pressure during the flip chip bonding process was set to 10 N larger than the pressure suggested from the ACP product. The above bonding procedure was conducted as a batch-process.

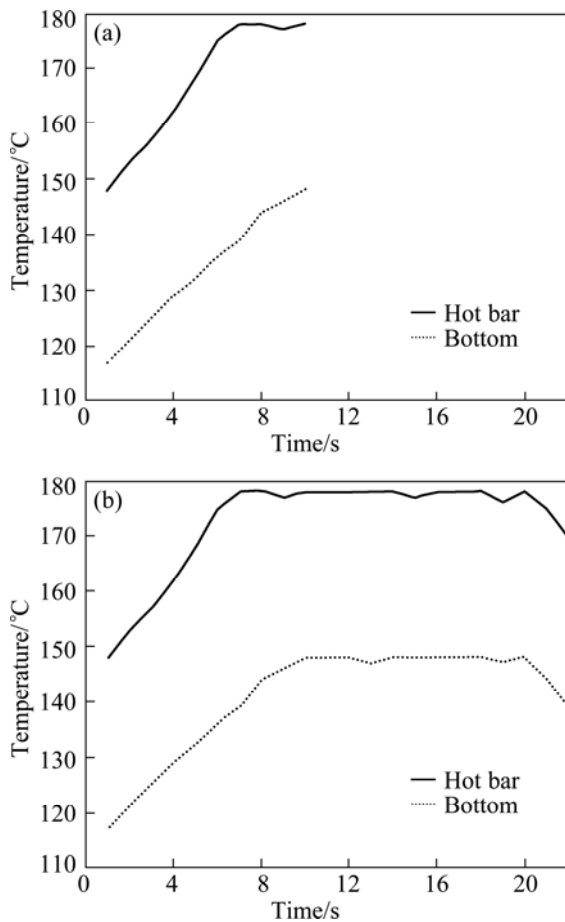


Fig.2 Bonding condition and temperature profile of RFID die as function of heating time: (a) 10 s for heating; (b) 20 s for heating

2.3 Shear bonding strength

The shear bonding strength was measured on the bonded die by using the shear tester (model: Dage 4 000,

Dage, USA) as a function of process condition. The bottom of the shearing tool was located 50 μm above the substrate and the speed of the shearing tool was 167 $\mu\text{m/s}$. The shear strength was determined from the average out of 10 measurements for each process condition. The fractural surface was observed from the optical microscope to identify the crack propagation path.

2.4 Recognition distance of tag

The materials for antenna pattern, bonding time, and aging time at room temperature can change the performance of RFID inlay. Therefore, this study measured the recognition distance of RFID inlay as a function of process conditions in an anechoic chamber. The RFID inlay was stuck to the stand and the stand was located apart from the reader in a crow line. The distance apart from the stand to the reader was increased to 10 mm step.

3 Results and discussion

Figure 3 shows the exothermal peaks during curing as a function of ACP materials and heating rate (1–15

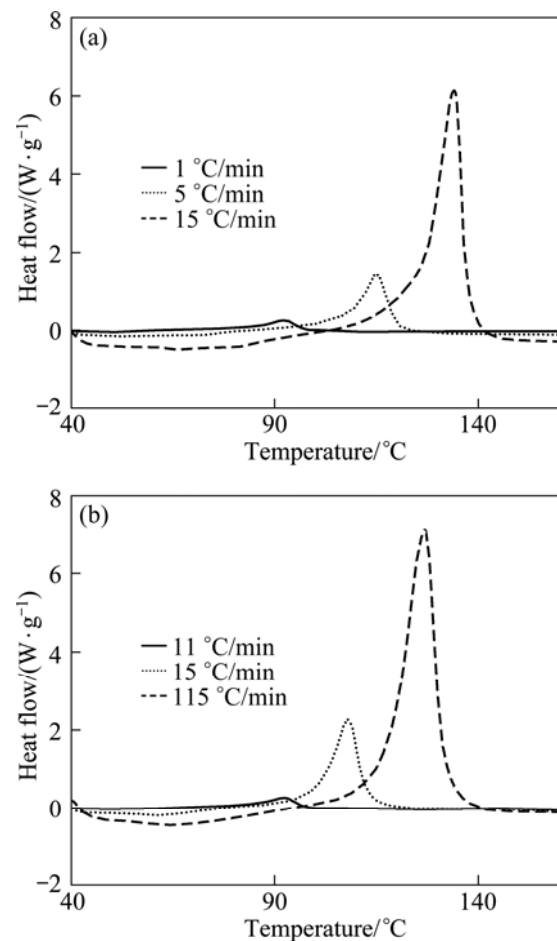


Fig.3 DSC curves of ACP materials with different heating rates: (a) ACP-1; (b) ACP-2

°C/min). As the curing rate increased from 1 °C/min to 15 °C/min, neither ACP-1 and nor ACP-2 showed noticeable exothermal peak near to 150 °C. For the same ACP material, however, the temperatures of the exothermal peaks and the total caloric value increased with the heating rate. The real bonding process by using the hot bar and bottom plate in this study indicated very rapid heating rate as observed in Fig.2. As the heating rate comes to real bonding condition, therefore, curing will occur at once due to an explosive increase of exothermal peaks above 150 °C. Comparing with ACP-1 for the constant heating rate, ACP-2 had a lower temperature of exothermal peak, indicating a faster hardening rate as indicated in Table 1. For the reason, ACP-1 was determined the bonding time condition as 5, 10, and 15 s; ACP-2 was fixed the condition as 4, 9, and 14 s.

As the heating rate decreased significantly to 1 °C/min, the exothermal peak appeared at low temperature, i.e. approximately 90 °C. For the reason, it is plausible to expect the exothermal peak at room temperature, although the heating rate approaches to zero. This means that the rapid curing ACP materials cannot avoid the unexpected hardening at room temperature. In fact, the ACP materials in the study have a limited storage life even at room temperature, e.g. 2 weeks for ACP-1 and 1 week for ACP-2 as shown in Table 1.

Table 2 summarizes the behavior of the shear bonding strength and fracture surface as a function of antenna material and bonding time for ACP-1. The maximum shear strength was measured at the optimized bonding time, i.e. 10 s for this study, regardless of antenna materials. For the lack of bonding time, i.e. 5 s for this study, the dominant fractures were delamination at the interface between ACP and antenna/PET due to insufficient hardening. However, for the excess bonding time, i.e. 15 s for this study, the shear strength decreased due to the thermal degradation of ACP material. For the optimized and excess bonding time, the fracture mode in the antenna material made by Ag ink indicated the delamination of antenna pattern as shown in Fig.4. The adhesion of Ag ink to PET seemed to be insufficient when the ACP was sufficiently hardened.

The shear strength of antenna pattern made by Ag ink was 13%–14% larger than that made by Cu-foil. This is probably due to the anchor effect of Ag pattern as induced from the cross-section in Fig.5 and from the fractured surface in Fig.4. Figs.5(a) and (c) show the cross-section of flip-chip joint made by Cu-foil antenna. Figs.5(b) and (d) indicate the cross-section of joint made by Ag ink. The thickness of Ag ink antenna was approximately 5 μm, i.e. 1/7 times of Cu antenna thickness.

Table 2 Shear strength and fracture surface as function of antenna materials and hardening conditions for ACP-1

Antenna pattern material	Heating time/s	Shear strength/N	Fractured path	Bonding quality
Cu foil	5	4.1	①	Insufficient hardening
	10	15.7	①, ②	Optimized condition (Fractured evenly along all interfaces)
	15	12.8	②	Degradation of ACP and bonding strength due to over-hardening
Paste type Ag ink	5	4.9	①	Insufficient hardening
	10	17.7	①, ③	Optimized condition
	15	14.6	①, ③	Degradation of ACP and bonding strength due to over-hardening

① Interface delamination at ACP and antenna/PET; ② Interface delamination at ACP and die; ③ Delamination of antenna pattern

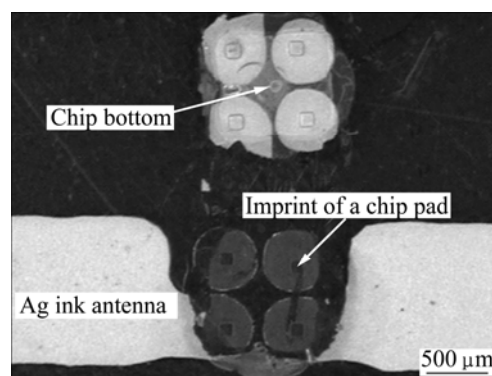


Fig.4 Representative shear fractured surface for paste-type Ag ink antenna(15 s curing for ACP-1)

The RFID chips were bonded by thermo-compression process, therefore deforming the filler materials easily and then influencing the antenna material sequentially. During the process, the Cu pattern antenna was sustainable to the local strain near the Au bumps, therefore producing the large radius of bending curvature within the elastic deformation range[9]. Regardless of filler composition, on the other hand, the Ag antenna produced the local plastic deformation and finally the protrusion was near the bonding joint[9]. Post to the bonding process, the bumps of die were observed to be impressed to the interior of antenna pattern. This geometry should increase the shear strength due to the anchor effect. There is more secure evidence to explain the anchor effect for the Ag ink antenna. Figure 4 shows a clear trace of Au bumps on the PET surface. The protrusion of Ag antenna showed different shapes as shown in Figs.5(b) and (d). This irregular protrusion shape can vary the insulation distance between the RFID die and antenna pattern, changing the RF characteristics inconsistent. Therefore, it is necessary to minimize the variation of protrusion shape for producing the

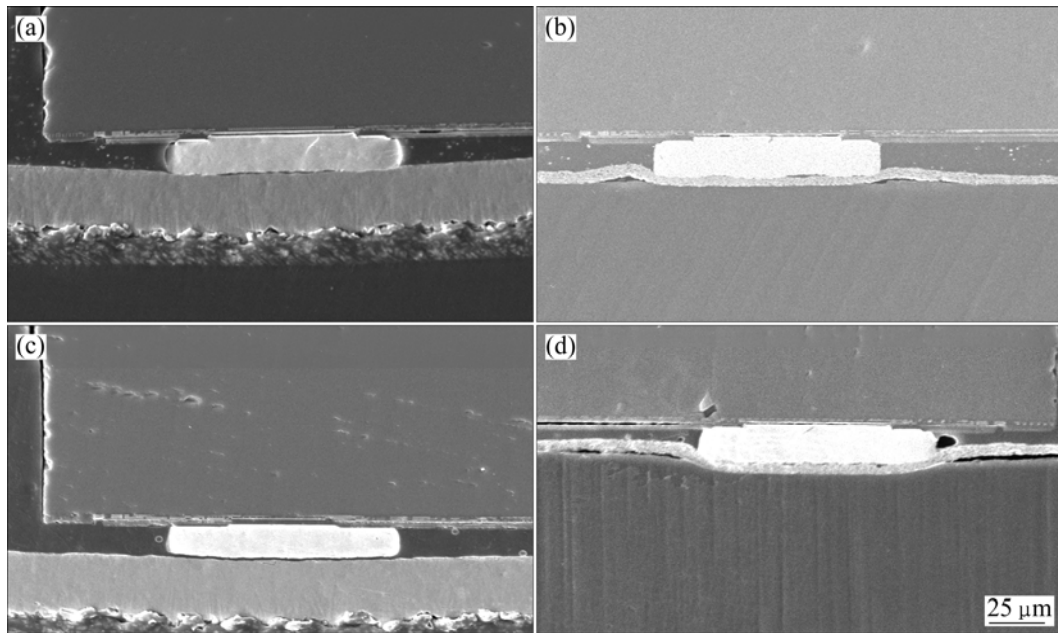


Fig.5 Cross-section images of joints with respect to antenna materials and ACP: (a) Round shape Ag fillers on Cu antenna; (b) Round shape Ag fillers on Ag ink antenna; (c) Au/Ni coated polymer fillers on Cu antenna; (d) Au/Ni coated polymer fillers on Ag ink antenna

homogeneous performance of RFID inlay[20].

Table 3 summarizes the behavior of shear bonding strength and fracture surface as a function of antenna material and bonding time for ACP-2. The bonding time was optimized with a variation of shear strength. As indicated in Table 1 and Fig.3, ACP-2 has a faster time for the optimized curing and a larger shear strength than ACP-1 by 25%–29%. For the reason, ACP-2 has a superior adhesion property than ACP-1. However, ACP-2 shows a similar trend with ACP-1 that the shear bonding strength is decreased continuously after the optimum bonding time is achieved. Furthermore, the Ag antenna with ACP-2 has a shear strength larger than the Cu antenna by 10%–16% due to the anchor effect of Ag pattern.

Figure 6 shows the variation of recognition distance for RFID inlays as a function of ACP/antenna materials, bonding time and aging time at room temperature. On the whole, the measured recognition distance was significantly shorter than that for the commercialized. This was probably because a design of antenna pattern was not optimized as that for the commercialized. However, there was no problem to compare the effects of the applied materials and bonding conditions on the variation of recognition distance. Focusing on the aging time to 1 week, the stable recognition distance was measured under the curing condition above 10 s for ACP-1 and above 4 s for ACP-2. However, the Ag antenna with ACP-2 indicated the shortest recognition distance.

Table 3 Shear strength and fracture surface as function of antenna materials and hardening conditions for ACP-2

Antenna pattern material	Heating time/s	Shear strength/N	Fractured path	Bonding quality
Cu foil	4	19.6	①, ②, ③	Optimized condition (Fractured evenly along all interfaces)
	9	18.0	①, ②, ③	Degradation of ACP and bonding strength due to over-hardening
	14	14.9	①, ②	Degradation of ACP and bonding strength due to over-hardening
Paste type Ag ink	4	22.8	①, ③	Optimized condition
	9	19.7	①, ③	Degradation of ACP and bonding strength due to over-hardening
	14	17.3	①, ③	Degradation of ACP and bonding strength due to over-hardening

① Interface delamination at ACP and antenna/PET; ② Interface delamination at ACP and die; ③ Delamination of antenna pattern

The Cu antenna with ACP-1 showed an abrupt decrease of recognition distance as the aging time approached to 1 month at room temperature. This phenomenon is probably explained from the cross-section image of joint as shown in Fig.5(a). After

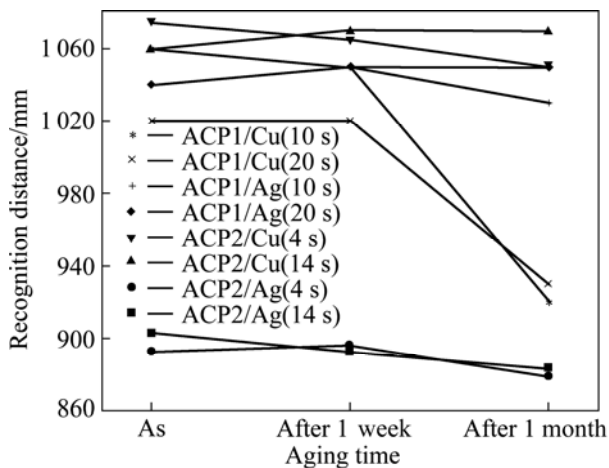


Fig.6 Variation of recognition distance for RFID inlays with respect to ACP/antenna materials, hardening time and aging time at room temperature

bonding process, the thick Cu antenna produced the elastic bending deformation. During the aging at room temperature, the curvature of Cu antenna might be affected by a stress and stretched out to flat surface. Conclusively, the stress relieve acting on the Cu antenna decreased the contacting area of conductive fillers, and reduced the recognition distance significantly after the specific aging time was reached. On the other hand, the plastic deformation occurred at the joint of the Ag antenna during the bonding process. Therefore, the Ag antenna joint was comparatively stabilized with respect to the aging. For the Cu antenna, the use of polymer cored fillers (ACP-2) suppressed significantly the decrease of recognition distance because of its elasticity and dynamic stability. The elasticity of the polymer cored fillers also reduced the bending of Cu antenna for die bonding process. Comparing Fig.5(a) with (c), the polymer cored fillers showed a less bending of Cu antenna, restraining a decrease of contacting area because of the dynamic stability. The Ag ink antenna showed an excellent long-term reliability, compared with the Cu antenna.

4 Conclusions

1) This study investigated the reliability of the flip-chip joint in which ACP was used on the PET substrate. RFID dies were flip-chip bonded by using ACP.

2) Regardless of antenna materials, there was an optimized time for bonding to obtain the maximum shear strength. Insufficient, and excess bonding time decreased the shear strength. Anchor effect of the antenna made by

Ag ink produced the larger shear strength than that made by Cu-foil.

3) During the die bonding process, the bending of Cu antenna was observed and the phenomenon decreased the long-term reliability of recognition distance in the case of use of ACP containing Ag-fillers.

Acknowledgements

This work was supported by the Ministry of Commerce, Industry and Energy (MOCIE) of Korea (10031777).

References

- [1] BANKS J, HANNY D, PACHANO M A, THOMPSON L J. RFID Applied John [M]. New Jersey: Wiley & Sons, 2007, 299–305.
- [2] CHENG C M, BUFFA V, O'HARA W, XIA B, SHAH J. Low cost, high speed reel-to-reel RFID tag assembly[J]. Global SMT & Packaging, 2005, 5: 17–21.
- [3] FAIRLEY M. RFID Smart Labels [M]. London: Tarsus Exhibition and Publishing, 2005, 19.
- [4] LU D Q, TONG Q K, WONG C P. Conductivity mechanisms of isotropic conductive adhesives (ICAs) [J]. IEEE Transactions on Electronics Packaging Manufacturing, 1999, 22(3): 223–227.
- [5] WOJCIECHOWSKY D, VANFLETEREN J, REESE E, HAGEDORN H W. Electro-conductive adhesives for high density package and flip-chip interconnections[J]. Microelectronics Reliability, 2000, 40: 1215–1226.
- [6] RASUL J S. Chip on paper technology utilizing anisotropically conductive adhesive for smart label applications [J]. Microelectronics Reliability, 2004, 44: 135–140.
- [7] YIN C, LU H, BAILEY C, CHAN Y C. Effects of solder reflow on the reliability of flip-chip on flex interconnections using anisotropic conductive adhesives [J]. IEEE Transactions on Electronics Packaging Manufacturing, 2004, 27(4): 254–259.
- [8] CHIN M, IYER K A, HU S J. Prediction of electrical contact resistance for anisotropic conductive adhesive assemblies [J]. IEEE Transactions on Components and Packaging Technologies, 2004, 27(2): 317–326.
- [9] TEO M, MHAISALKAR S G, WONG E H, TEO P S, WONG C C, ONG K, GOH C F, TEH L K. Correlation of material properties to reliability performance of anisotropic conductive adhesive flip chip packages [J]. IEEE Transactions on Components and Packaging Technologies, 2005, 28(1): 157–164.
- [10] KAY R W, STOYANOV S, GLINSKI G P, BAILEY C, DESMULLIEZ M P Y. Ultra-fine pitch stencil printing for a low cost and low temperature flip-chip assembly process[J]. IEEE Transactions on Components and Packaging Technologies, 2007, 30(1): 129–136.
- [11] NICOLICS J, MÜNDLEIN M. Micro- and Opto-electronic materials and structures[M]. New York: Springer Science and Business Media, 2007, 571–593.
- [12] SUHIR E, LEE Y C, Wong C P. Micro- and opto-electronic materials and structures[M]. New York: Springer Science and Business Media, 2007, 527–228.
- [13] ABAD E, MAZZOLAI B, JUARROS A, GOMEZ D, MONDINI A, SAYHAN I, KRENKOW A, BECKER T. Investigation of fabrication

- and encapsulation processes for a flexible tag microlab[J]. *Microsystem Technologies*, 2008, 14: 527–534.
- [14] TENG K F, VEST R W. Application of ink jet technology on photovoltaic metallization [J]. *Electron Device Letters*, 1988, 9(11): 591–593.
- [15] HOLMAN R K, UHLAND S A, CIMA M J, SACHS E. Surface adsorption effects in the inkjet printing of an aqueous polymer solution on a porous oxide ceramic substrate [J]. *Journal of Colloid and Interface Science*, 2002, 247(2): 266–274.
- [16] RYU B H, CHOI Y, PARK H S, BYUN J H, KONG K, LEE J O, CHANG H. Synthesis of highly concentrated silver nanosol and its application to inkjet printing [J]. *Colloid and Surfaces A*, 2005, 270–271: 345–351.
- [17] LIU Z, SU Y, VARAHRAMYAN K. Inkjet-printed silver conductors using silver nitrate ink and their electrical contacts with conducting polymers [J]. *Thin Solid Films*, 2005, 478: 275–279.
- [18] LEE J H, YU A M, KIM J H, KIM M S, KANG N. Reaction properties and interfacial intermetallics for Sn-xAg-0.5Cu solders as a function of Ag content [J]. *Metals and Materials International*, 2008, 14(5): 649–654.
- [19] YIM M J, PAIK K W. Recent advances on anisotropic conductive adhesives (ACAs) for flat panel displays and semiconductor packaging applications [J]. *International Journal of Adhesion and Adhesives*, 2006, 26: 304–313.
- [20] NAOKI I, SHUNJI B, HIDEHIKO K, HIROSHI K, SHUNICHI K. RFID tag, modular component and RFID tag manufacturing method. Japanese patent Pub. No. 2006260205, Japanese Patent Appl. No. 2005077108[P].
- [21] NORTON D P, HEO Y W, IVILL M P, IP K, PEARTON S J, CHISHOLM M F, STEINER T. ZnO: growth, doping and processing [J]. *Materials Today*, 2004, 7(6): 34–40.

(Edited by HE Xue-feng)